Modal Matching for LPV Model Reduction of Aeroservoelastic Vehicles

Julian Theis*
Hamburg University of Technology, Hamburg, 21073, Germany
Béla Takarics†, Harald Pfifer† and Gary Balas‡
University of Minnesota, Minneapolis, MN 55455, USA
Herbert Werner§
Hamburg University of Technology, Hamburg, 21073, Germany

A model order reduction method is proposed for models of aeroservoelastic vehicles in the linear parameter-varying (LPV) systems framework, based on state space interpolation of modal forms. The dynamic order of such models is usually too large for control synthesis and implementation since they combine rigid body dynamics, structural dynamics and unsteady aerodynamics. Thus, model order reduction is necessary. For linear time-invariant (LTI) models, order reduction is often based on balanced realizations. For LPV models, this requires the solution of a large set of linear matrix inequalities (LMIs), leading to numerical issues and high computational cost. The proposed approach is to use well developed and numerically stable LTI techniques for reducing the LPV model locally and then to transform the resulting collection of systems into a consistent modal representation suitable for interpolation. The method is demonstrated on an LPV model of the body freedom flutter vehicle, reducing the number of states from 148 to 15. The accuracy of the reduced order model (ROM) is confirmed by evaluating the ν-gap metric with respect to the full order model and by comparison to another ROM obtained by state-of-the-art LPV balanced truncation techniques.

I. Introduction

Weight reduction is one of the primary objectives of aircraft design, leading to increased fuel efficiency and hence to reduced operating costs and environmental impact. As an adverse consequence of decreased structural mass, the natural frequencies of structural modes are lowered. This can cause undesired coupling of rigid body dynamics and elastic deformation through aerodynamic forces and result in a dynamic instability known as body freedom flutter. Additionally, coupling between structural deformation and reactive forces from actuator usage needs to be considered in design. The interaction of structural dynamics, aerodynamics and controls is termed aeroservoelasticity and is receiving increased attention throughout the aerospace community in the last years.[1–3]

Active aeroservoelastic control is becoming increasingly important for future large aircraft to counter adverse effects on stability and handling qualities. Designing controllers for this task requires models that include rigid body motion, structural modes, and unsteady aerodynamic effects. Such models are of high dynamic order and need to capture the varying dynamics across the flight envelope. Linear parameter-varying (LPV) systems[4,5] provide a natural modeling framework for aeroservoelastic control. LPV systems are linear dynamic systems that depend continuously on external operating conditions. A rich theory exists, that allows parts of the linear robust control theory to be applied to this special class of nonlinear systems. The high order of aeroservoelastic models, however, prohibits their immediate use in conjunction with modern LPV

*Graduate Research Assistant, Institute of Control Systems, email: julian.theis@tuhh.de
†Post-Doctoral Associate, Aerospace Engineering and Mechanics Department, email: {btakaric,hpfifer}@umn.edu
‡Professor, Aerospace Engineering and Mechanics Department, email: balas@aem.umn.edu
§Professor, Institute of Control Systems, email: h.werner@tuhh.de

control synthesis techniques, whose complexity scales badly with the model order. It is therefore necessary to obtain reduced order LPV models that are suitable for control design.

In practice, the continuum of operating conditions is commonly approximated by a finite number of operating points. The collection of linear time invariant (LTI) models obtained from evaluating an LPV system for these parameters is called a grid representation. Model order reduction techniques for gridded LPV systems were developed in Ref. 6 and require the computationally expensive solution of a large set of linear matrix inequalities (LMIs). The approach is hence limited to systems with low dynamic order. It was recently successfully applied in Ref. 7, but the study also revealed severe numerical problems and the need for heuristic pre-processing.

The aim of the present paper is therefore to introduce an alternative approach to model order reduction of gridded LPV systems by using LTI techniques. In a first step, the LTI systems at each grid point are individually reduced, resulting in different state space bases for each reduced order model (ROM). In a second step, the ROMs are transformed into a canonical modal form, recovering an approximately consistent state space basis for all models. This state space representation is suitable for interpolation and hence allows to define an LPV model with a reduced number of states that approximates the original system. After briefly reviewing preliminaries about model order reduction and LPV systems in Section II, the novel approach is described in Section III. The proposed model order reduction procedure is applied to a small flexible aircraft, introduced in Section IV. In this section, the ROMs obtained with the proposed approach are shown to indeed form a gridded LPV system that accurately approximates the original LPV model. The results are further compared to the LMI-based reduction proposed in Ref. 7.

II. Model Order Reduction for Linear Parameter-Varying Systems

An LPV system is described by the state space model

$$\dot{x}(t) = A(\rho(t))\ x(t) + B(\rho(t))\ u(t)\ , \tag{1a}$$
$$y(t) = C(\rho(t))\ x(t) + D(\rho(t))\ u(t)\ , \tag{1b}$$

with the continuous matrix functions $A\colon \mathcal{P} \to \mathbb{R}^{n_x \times n_x}$, $B\colon \mathcal{P} \to \mathbb{R}^{n_x \times n_u}$, $C\colon \mathcal{P} \to \mathbb{R}^{n_y \times n_x}$, $D\colon \mathcal{P} \to \mathbb{R}^{n_y \times n_u}$, the state $x\colon \mathbb{R} \to \mathbb{R}^{n_x}$, input $u\colon \mathbb{R} \to \mathbb{R}^{n_u}$, output $y\colon \mathbb{R} \to \mathbb{R}^{n_y}$ and a time-varying scheduling signal $\rho\colon \mathbb{R} \to \mathcal{P}$, where $\mathcal{P}$ is a compact subset of $\mathbb{R}^{n_\rho}$. In a grid representation, the LPV system is described as a collection of LTI models $(A_k,\, B_k,\, C_k,\, D_k) = (A(\rho_k), B(\rho_k), C(\rho_k), D(\rho_k))$ obtained from evaluating the LPV model at a finite number of parameter values $\{\rho_k\}_1^{n_{\text{grid}}} = \mathcal{P}_{\text{grid}} \subset \mathcal{P}$. For brevity, the explicit dependence on time is dropped from this point on.

A. Reduction Methods

The aim of model order reduction is to approximate the input-output behavior of a given system with a model of lower dynamic order. The first step is to partition the dynamic system (1) as

$$\dot{x}_1 = A_{11}(\rho)\ x_1 + A_{12}(\rho)\ x_2 + B_1(\rho)\ u\ , \tag{2a}$$
$$\dot{x}_2 = A_{21}(\rho)\ x_1 + A_{22}(\rho)\ x_2 + B_2(\rho)\ u\ , \tag{2b}$$
$$y = \ C_1(\rho)\ x_1 + \ C_2(\rho)\ x_2 + \ D(\rho)\ u\ , \tag{2c}$$

by changing the basis of the state space. This is discussed in section II.B. Given Eq. (2), there are essentially two different ways of removing x_2 from the state vector: truncation and residualization.[8,9]

1. *Truncation*

Truncation refers to simply discarding x_2 from the dynamic system, i. e., the ROM is

$$\dot{x}_1 = A_{11}(\rho)\, x_1 + B_1(\rho)\, u\ , \tag{3a}$$
$$y = \ C_1(\rho)\, x_1 + \ D(\rho)\, u\ . \tag{3b}$$

Model reduction by truncation is preferred when accuracy of the reduced order model at high frequencies is required. Truncation exactly preserves the feedthrough term $D(\rho)$ and hence the truncated model equals the full order model at infinite frequency.

2. Residualization

The second method to remove states from a system is residualization, i. e., to set $\dot{x}_2 = 0$. Solving for x_2 and substituting into Eq. (2) then yields the ROM

$$\dot{x}_1 = \left(A_{11}(\rho) - A_{12}(\rho)\, A_{22}^{-1}(\rho)\, A_{21}(\rho)\right)\, x_1 + \left(B_1(\rho) - A_{12}(\rho)\, A_{22}^{-1}(\rho)\, B_2(\rho)\right)\, u\,, \tag{4a}$$

$$y = \left(C_1(\rho) - C_2(\rho)\, A_{22}^{-1}(\rho)\, A_{21}(\rho)\right)\, x_1 + \left(D(\rho) - C_2\,(\rho) A_{22}^{-1}(\rho)\, B_2(\rho)\right)\, u\,. \tag{4b}$$

Residualization preserves the steady-state gain of the system and hence retains accuracy at low frequencies.

B. State Transformations for Reduction

1. Modal Decomposition

For LTI systems, modal decomposition allows to remove modes below or above the frequency range of interest without affecting other modes of the system and is therefore most useful when physical insight into the problem is available. For example, removing the phugoid mode of an aircraft is a common simplification made in the design of controllers concerned with short period dynamics. Another important application of this form for model order reduction is the decomposition of a system into a stable and an antistable part. An LTI system in modal form is described by

$$\dot{x} = \begin{bmatrix} A_1 & 0 & & \\ 0 & A_2 & \ddots & \\ & \ddots & \ddots & 0 \\ & & 0 & A_n \end{bmatrix} x + \begin{bmatrix} B_1 \\ B_2 \\ \vdots \\ B_n \end{bmatrix} u\,, \tag{5a}$$

$$y = \begin{bmatrix} C_1 & C_2 & \cdots & C_n \end{bmatrix} x + D\, u\,, \tag{5b}$$

where

$$A_i = \begin{bmatrix} \Re(\lambda_i) & \Im(\lambda_i) \\ -\Im(\lambda_i) & \Re(\lambda_i) \end{bmatrix} \tag{6}$$

for complex conjugate eigenvalues $\lambda_i = \Re(\lambda_i) \pm \mathrm{j}\, \Im(\lambda_i)$ and $A_i = [\lambda_i]$ for real eigenvalues. Although the state space matrix A in Eq. (5a) is in Jordan real canonical form, the dynamic system is not in a canonical form since any block diagonal state transform that commutes with the Jordan blocks (i. e., any block-diagonal matrix with blocks of the form $\left[\begin{smallmatrix} a & -b \\ b & a \end{smallmatrix}\right]$) will preserve the matrix A while altering the basis of the state space. The modal form given in Eq. (5) is thus not unique.

The modal form depends on a state transformation spanning the eigenspace of the system matrix A. Precisely, the transformation matrix that converts a system to modal form is

$$T_{\mathrm{mod}}^{-1} = \begin{bmatrix} \Re(v_1) & \Im(v_1) & \Re(v_2) & \Im(v_2) & \cdots & \Re(v_n) & \Im(v_n) \end{bmatrix}\,, \tag{7}$$

where v_i are the eigenvectors corresponding to the eigenvalues λ_i. For LPV systems, eigenvalues and eigenvectors of the parameter-dependent matrix $A(\rho)$ are also parameter-dependent and hence the transformation into modal form would also depend on the parameters, see Ref. 6 for a thorough discussion. The use of parameter-varying transformations introduces an explicit dependence on the parameter variation rate into the differential equation that governs the system dynamics. For a change of coordinates $\xi(t) = T(\rho(t))\; x(t)$, the state space model (1) becomes

$$\dot{\xi} = \left(T(\rho)\, A(\rho)\, T^{-1}(\rho) + \frac{\partial T(\rho)}{\partial \rho}\, T^{-1}(\rho)\, \dot{\rho}\right)\, \xi + T(\rho)\, B(\rho)\, u\,, \tag{8a}$$

$$y = C(\rho)\, T^{-1}(\rho)\, \xi + D(\rho)\, u. \tag{8b}$$

The term $\frac{\partial T(\rho)}{\partial \rho}\, T^{-1}(\rho)\, \dot{\rho}$ in Eq. (8a) may produce large off-diagonal elements for non-zero rates. Consequently, the decoupled structure of Eq. (5a) is in general not attained. There are essentially two remedies for this problem. The first is to apply a parameter-independent transformation that yields modal form at a

single grid point and then to neglect the modal coupling at the other grid points while removing modes from the LPV system. This can severely diminish the usefulness of a modal form, where achieving decoupling is the primary goal. The second is to neglect the term $\frac{\partial T(\rho)}{\partial \rho} T^{-1}(\rho)\,\dot{\rho}$ which results in an unknown amount of inconsistency in the state vector across the parameter space. For gridded LPV systems, an additional challenge with this approach is to identify and associate the modes at each grid-point since, as pointed out before, a modal state space basis calculated for an individual LTI model is not unique.

2. Balanced Realization

A balanced realization refers to a state space realization whose states are each equally controllable and observable. These measures are provided by the controllability and observability Gramians[10] that, for LPV systems, are defined as symmetric positive definite matrix functions $P(\rho) = P^T(\rho) \succ 0$ and $Q(\rho) = Q^T(\rho) \succ 0$ such that $\forall \rho \in \mathcal{P}$, the following Lyapunov inequalities hold;

$$\frac{\mathrm{d}}{\mathrm{d}t}P(\rho) + A(\rho)\ P(\rho) + P(\rho)\ A^T(\rho) + B(\rho)\ B^T(\rho) \prec 0, \tag{9a}$$

$$\frac{\mathrm{d}}{\mathrm{d}t}Q(\rho) + A^T(\rho)\ Q(\rho) + Q(\rho)\ A(\rho) + C^T(\rho)\ C(\rho) \prec 0. \tag{9b}$$

The expression $X \prec (\succ)\ 0$ denotes negative (positive) definiteness of a symmetric matrix X. A computational solution of the inequalities (9) requires to approximate $\mathcal{P}$ by $\mathcal{P}_{\text{grid}}$ and further to predefine the parameter dependence of P and Q, see Ref. 6. For LTI systems, unique Gramians can be explicitly calculated from the Lyapunov equations

$$A\,P + P\,A^T + B\,B^T = 0, \tag{10a}$$

$$A^T Q + Q\,A + C^T C = 0. \tag{10b}$$

In a balanced realization, the controllability and observability Gramians are equal and diagonal, denoted by $\hat{P} = \hat{Q} = \Sigma$. The matrix Σ contains the Hankel singular values of the system on its diagonal, from which the combined controllability and observability of each state can be inferred. Small Hankel singular values indicate that a state can be removed from the model without significantly altering the input-output properties, making the balanced transformation extremely useful for model order reduction. The balancing state transformation T_{bal} is found from $\hat{P} = T_{\text{bal}}\,P\,T_{\text{bal}}^T$ and $\hat{Q} = (T_{\text{bal}}^{-1})^T\,Q\,T_{\text{bal}}^{-1}$. To avoid the rate dependence introduced by parameter-dependent transformations, P and Q are commonly chosen to be parameter-independent even for LPV systems.

III. Local Reduction and Modal Matching

In contrast to reducing the complete LPV model with parameter-independent transformations, the proposed approach is to reduce the LTI models at each grid point individually. This is called a local reduction. The resulting ROMs are then, again locally, transformed into a canonical state space representation. Finally, a reduced order LPV system is obtained through interpolation. Conceptually similar approaches are formulated, e. g., in Ref. 11–13.

A. Motivation

As discussed in section II.B.1, LPV systems cannot be transformed into modal form and hence physical insight into the problem is considerably harder to exploit. While it remains possible to simple discard, e. g., an altitude or velocity state, removing, a stability mode such as the spiral motion of an aircraft is not possible since the contributions from different physical states vary across the parameter space. The lack of a modal form also prohibits a stable/unstable decomposition of LPV systems. This is problematic for balanced truncation since the Lyapunov inequalities (9) that define the controllability and observability Gramians are solvable only if the system to be balanced is stable. A remedy is provided by a contractive coprime factorization,[6,7] which represents an unstable system as two stable input-output pairs. This factorization, as well as the balanced truncation itself, is not unique for LPV systems and requires to find feasible solutions to a large set of LMIs. This computationally challenging and numerically error-prone task scales badly with the dynamic order of the model and therefore its scope of application is limited to systems with a small number

of states. Model order reduction with this approach was pursued in Ref. 7 for an aeroservoelastic vehicle, where this limitation necessitated the use of heuristic pre-processing to reduce the number of states to 43 before a balanced truncation could be applied. Further, the restriction to parameter-independent Gramians was emphasized since otherwise the increase in computational complexity renders the problem intractable. Restricting the search to parameter-independent P and Q in inequalities (9), on the other hand, reduces the set of admissible solutions and might not yield the most useful realization for truncation. But even if it was permitted by available computational power to use parameter-dependent Gramians, they would still not be unique and the explicit dependence on parameter rates in the resulting ROM would in general not be desirable.

The proposed approach, on the contrary, allows well developed and numerically stable algorithms to be applied for local reductions. Stability modes can be easily removed using a modal decomposition and a stable/unstable decomposition can be performed in order to apply balanced truncation with unique Gramians. These local reductions, however, correspond to the use of a parameter-dependent transformation on the overall LPV system that takes different values at each grid point. It is hence expected to yield better results than the parameter-independent transformation calculated from the LMI approach. These advantages come at the price of an unknown approximation error caused by neglecting this parameter-dependence in the resulting ROM.

B. Local Model Reduction

The proposed local model reduction consists of three consecutive steps.

1. *Modal Truncation:* In a first step, the LTI models at the grid points are individually transformed into modal form and all modes below the frequency range of interest are removed by truncation. For aeroservoelastic vehicles, this eliminates rigid body motion and slow dynamics that are irrelevant for aeroservoelastic control.

2. *Modal Residualization:* Second, all modes above the frequency range of interest are residualized. This upper bound is typically determined by the available actuator bandwidth for aeroservoelastic vehicles. Modes that cannot be effectively controlled since they are outside of the control bandwidth are removed in this step. It is important to take into account the required frequency range for the controller to roll-off, i. e., the model should still be accurate slightly above the actuator bandwidth.

3. *Balanced Truncation:* Third, a stable/unstable decomposition is applied to the LTI models and the stable parts are individually transformed into a balanced realization. States are then truncated based on the Hankel singular values and the unstable part is added back. This step removes all states with minor contribution to the input/output behavior of the system and concludes the local reduction.

The result of this procedure is a collection of ROMs ($A_{k,\mathrm{red}}$, $B_{k,\mathrm{red}}$, $C_{k,\mathrm{red}}$, $D_{k,\mathrm{red}}$) that approximate the input-output behavior of the original LPV system at each grid point and that exactly preserve any unstable modes within the frequency range of interest. All LTI models are required to have the same order and the same number of complex and real poles (i. e., modes) in order for the next steps to be applicable.

C. Modal Matching

Having applied the local reduction, the input-output behavior of all local systems is consistent since the model reduction is performed at each grid point with the objective to preserve this characteristic. The internal representation of the dynamics—i. e., the basis of the state space—at different grid points may, however, vary as a consequence of the local reduction. Completely recovering consistency appears to be impossible since the individual balanced truncation operations are surjections, i. e. non-invertible projections into a lower dimensional subspace. The proposed method is thus to match modes with similar dynamic properties at neighboring grid points and to find a canonical representation that is expected to minimize the approximation error due to state inconsistency. To that end, the local systems are transformed into what will be referred to as a mode-wise canonical form. Starting from the modal form (5), each mode i at grid point k is individually transformed into the controller canonical form by calculating a transformation matrix $T_{k,i} = [\varphi_{k,i} \quad A_{k,i}^T \varphi_{k,i}]^T$, where $\varphi_{k,i}^T$ is the last row of $[b_{k,i} \quad A_{k,i}\, b_{k,i}]^{-1}$ and $b_{k,i}$ is the first non-zero column

of $B_{k,i}$, see Ref. 14 for the detailed procedure. Applying this transformation, the state space matrices of the ith oscillatory[a] mode at grid point k become

$$\underbrace{T_{k,i}\,A_{k,i}\,T_{k,i}^{-1}}_{\underline{A}_{k,i}} = \begin{bmatrix} 0 & 1 \\ -\omega_{k,i}^2 & -2\,\omega_{k,i}\,\zeta_{k,i} \end{bmatrix}, \quad \underbrace{T_{k,i}\,B_{k,i}}_{\underline{B}_{k,i}} = \begin{bmatrix} 0 & \star & \cdots & \star \\ 1 & \star & \cdots & \star \end{bmatrix}, \quad \underbrace{C_{k,i}\,T_{k,i}^{-1}}_{\underline{C}_{k,i}} = \begin{bmatrix} \star & \star \\ \vdots & \vdots \\ \star & \star \end{bmatrix}, \tag{11}$$

where $\omega_{k,i}$ is the natural frequency of the mode, $\zeta_{k,i}$ is the corresponding damping ratio and $\star$ denotes possible non-zero entries. The two states associated with a mode thus correspond to generalized displacement and generalized velocity and are normalized in magnitude and sign by the first column of the input matrix. The state space model at grid point k in this mode-wise canonical form is

$$\begin{bmatrix} \dot{x}_1 \\ \dot{x}_2 \\ \vdots \\ \dot{x}_n \end{bmatrix} = \begin{bmatrix} \underline{A}_{k,1} & 0 & & \\ 0 & \underline{A}_{k,2} & \ddots & \\ & \ddots & \ddots & 0 \\ & & 0 & \underline{A}_{k,n} \end{bmatrix} \begin{bmatrix} x_1 \\ x_2 \\ \vdots \\ x_n \end{bmatrix} + \begin{bmatrix} \underline{B}_{k,1} \\ \underline{B}_{k,2} \\ \vdots \\ \underline{B}_{k,n} \end{bmatrix} u\,, \tag{12a}$$

$$y = \begin{bmatrix} \underline{C}_{k,1} & \underline{C}_{k,2} & \cdots & \underline{C}_{k,n} \end{bmatrix} \begin{bmatrix} x_1 \\ x_2 \\ \vdots \\ x_n \end{bmatrix} + D_k\,u\,. \tag{12b}$$

Applying this transformation individually at two different grid points yields models that are described in different state space bases for essentially two reasons. First, the mode shapes change, hence the basis for the mode-wise canonical state space description in fact also varies across the parameter space. Second, variations in the plant's B matrix may lead to a different normalization of the states and therefore to inconsistency. Although, these issues imply that states at one grid point are not the same as at another, from physical considerations, the assumption that the dynamic properties and the related mode-shapes depend continuously on the parameters is reasonable. That is, a mode $(\underline{A}_{k,i}, \underline{B}_{k,i}, \underline{C}_{k,i})$ at one grid point k corresponds to a mode $(\underline{A}_{k+1,j}, \underline{B}_{k+1,j}, \underline{C}_{k+1,j})$ at a neighboring grind point $k+1$, on a sufficiently dense grid. The task is thus to "match" these modes in order to obtain a consistent state-space description of the gridded system that is suitable for interpolation. Within the mode-wise canonical representation of Eq. (12), this relates to identifying matching partial state vectors x_i and permuting them accordingly.

The key assumption of the modal matching approach is that modes which represent the same dynamic properties of the system at different grid points have similar characteristics as measured by the following four criteria:

1. the damped natural frequency $\bar{\omega}_{k,i} = |\lambda_{k,i}| = \sqrt{w_{k,i}^2 - \zeta_{k,i}^2}$
2. the damping ratio $\zeta_{k,i} = \arctan \frac{\Re(\lambda_{k,i})}{\Im(\lambda_{k,i})}$
3. the input direction $\operatorname{span}(\underline{B}_{k,i}^T)$
4. the output direction $\operatorname{span}(\underline{C}_{k,i})$

These criteria are combined into a matching function M_k, defined as

$$\begin{aligned} [M_k]_{i,j} = &\min\left(\frac{\bar{\omega}_{k,i}}{\bar{\omega}_{k+1,j}}, \frac{\bar{\omega}_{k+1,j}}{\bar{\omega}_{k,i}}\right)^{\alpha} + \min\left(\frac{\zeta_{k,i}}{\zeta_{k+1,j}}, \frac{\zeta_{k+1,j}}{\zeta_{k,i}}\right)^{\alpha} \\ &+ \left(\frac{|\left\langle \underline{B}_{k,i}, \underline{B}_{k+1,j} \right\rangle_F|}{\|\underline{B}_{k,i}\|_F \, \|\underline{B}_{k+1,j}\|_F}\right)^{\alpha} + \left(\frac{|\left\langle \underline{C}_{k,i}, \underline{C}_{k+1,j} \right\rangle_F|}{\|\underline{C}_{k,i}\|_F \, \|\underline{C}_{k+1,j}\|_F}\right)^{\alpha}, \end{aligned} \tag{13}$$

where $\langle X, Y \rangle_F = \operatorname{trace}\left(X^T Y\right) = \operatorname{trace}\left(Y^T X\right)$ is the Frobenius scalar product, $\|X\|_F = \sqrt{\langle X, X \rangle_F}$ is the Frobenius norm, and $\alpha \geq 1$ is a free parameter to adjust the matching function. The first two terms compare

[a]For non-oscillatory modes corresponding to a single real pole, analog considerations apply.

natural frequency and damping ratio, the last two the alignment of input and output directions. Each of the four terms equals one if the two compared modes are identical and is less than one if they differ. The parameter α determines how sensitive the matching function is to variations of the characteristics; a larger value can help to separate close-by modes. For the application considered in this paper, $\alpha = 2$ yielded consistently satisfying results. Each row of the matching function corresponds to a mode at grid point k while each column represents a mode at grid point $k+1$. Large values $[M_k]_{i,j}$ are then an indicator for the ith mode at grid point k to correspond to the jth mode at grid point $k+1$. Consequently, the permutation index is calculated from determining the column of the matching function with the largest matching value for each row. If multiple modes of grid point k are assigned to the same mode at grid point $k+1$, the ratio of the respective matching values is calculated and the largest value across all modes that are not assigned yet is used to resolve the double assignment. The modes are eventually permuted such that matching modes are in the same order for all local models throughout the parameter space.

The states at neighboring grid points are thus constructed to capture the same dynamic properties of the system. Though technically still different from each other, an approximately consistent state space representation is obtained. In that sense, the variation of the unknown parameter-dependent transformation—and hence the approximation error due to neglecting this dependence—is minimized. It should be emphasized that the matching algorithm is deterministic and if applied twice to the same system results in the same ordering of the modes. Further, the representation given in Eq. (12) is numerically well conditioned.

IV. Example: Model Reduction for the Body Freedom Flutter Vehicle

The Body Freedom Flutter Vehicle (BFF) is a test platform developed by the U.S. Air Force Research Laboratory and Lockheed Martin Aeronautics Company for the investigation of aeroservoelastic effects and demonstration of active aeroservoelastic control.[15] It has been donated to the Unmanned Aerial Vehicle laboratories of the University of Minnesota[b]. Figure 1 shows a schematic of the vehicle. For the present paper, six accelerometers are considered as measurement devices; two located at each wing tip and two in the center body. The two body flaps and two outboard flaps are used as control inputs.

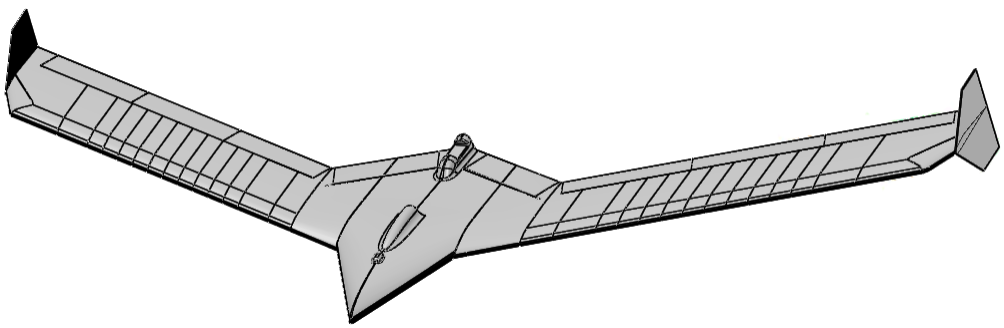

Figure 1. Body Freedom Flutter Vehicle

A set of 21 linear models parameterized by equivalent airspeed from 40 to 80 knots in steps of 2 knots is used as a starting point. The models represent straight level flight at 1000 ft altitude. The airframe model, excluding sensor and actuator models, has 148 states. The first 37 states represent generalized displacements related to 5 rigid body modes (lateral, plunge, roll, pitch and yaw), 8 flexible modes (symmetric and anti-symmetric bending and torsion) and 24 degrees of freedom associated with local vibrations of the control surfaces. The second 37 states are the corresponding generalized velocities and the remaining 74 states are associated with aerodynamic lags to approximate the rational function that describes the unsteady aerodynamics. All control surface actuators have a control bandwidth of 125 rad/s and the frequency range of interest for the BFF model reduction is defined to be 10–160 rad/s. Figure 2 shows the natural frequency and damping ratio of the short period dynamics and the elastic modes as a function of airspeed. Symmetric wing bending becomes unstable beyond 42 knots, followed by symmetric wing torsion beyond 60 knots and anti-symmetric wing torsion beyond 62 knots. Capturing these modes accurately in the ROM is vital for successful control design.

[b] http://www.uav.aem.umn.edu/

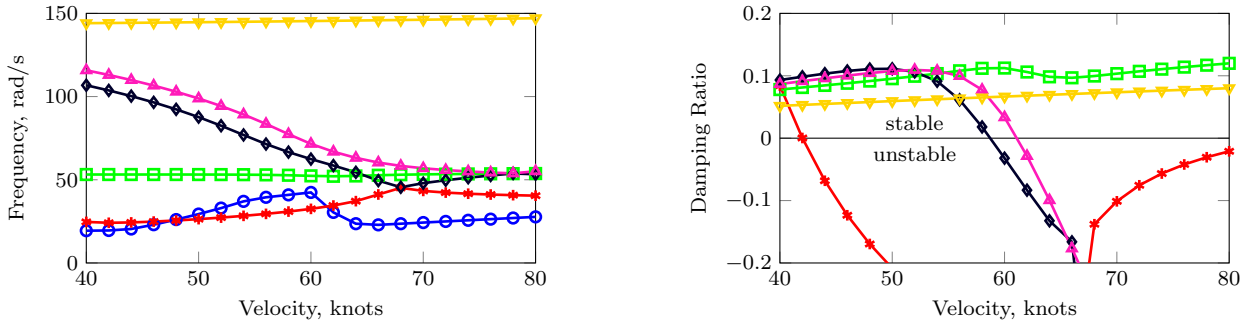

Figure 2. Velocity/frequency/damping (VFG) plot of the Body Freedom Flutter Vehicle.[7] Short period (—○—), 1st symmetric wing bending (—✱—), 1st anti-symmetric wing bending (—□—), 1st symmetric wing torsion (—◇—), 1st anti-symmetric wing torsion (—△—), 2nd anti-symmetric wing bending (—▽—).

A. Generation of the Reduced Order Models

1. Modal Matching Reduction

Following the steps proposed in section III.B, the 21 LTI models at the grid points are individually reduced. Truncating all modes below 10 rad/s removes 7 states and leads to models with 141 states each. Second, all modes above 200 rad/s are residualized. This removes 50 states and thus leads to models with 91 states each. Third, the Robust Control Toolbox' square root balanced truncation algorithm[16] `balancmr` is employed with a frequency weighting to define the region of interest as 10 rad/s to 200 rad/s, see figure 3(a). Based on the ν-gap metric (see section IV.B), 15 states are considered sufficient to keep the maximum value below 0.2 at 160 rad/s, see figure 3(b). The ROMs are then transformed into the mode-wise canonical form and the matching algorithm described in section III.C is applied.

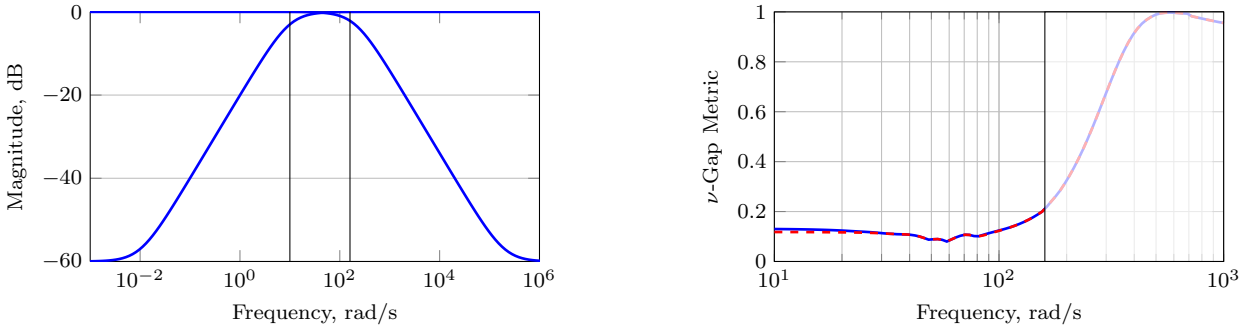

(a) Frequency weight for local balanced truncation

(b) Maximum ν-gap metric of 15 state model to 148 state model over the flight envelope evaluated at grid points (- - -) and at interpolation points (——)

Figure 3. Local Model Reduction.

2. LPV Model Reduction

To compare the proposed reduction method with state-of-the-art techniques, a reduced order LPV model of the BFF is generated by using a slightly modified version of the procedure developed in Ref 7. As a measure of which states to remove during pre-processing, the ν-gap metric is used. In a first step, all states that introduce a ν-gap less than 0.001 are residualized. Second, the states that change the ν-gap metric by less than 0.2 are truncated. Next, an approximate modal transformation is found by nonlinear optimization to minimize the ν-gap metric introduced by truncating all modes below 10 rad/s and residualizing all above 200 rad/s. The pre-processing results in a model with 42 states, which is then used for LMI-based balanced truncation. This eventually leads to a reduced order LPV model with 26 states.

B. Comparison of the Reduced Order Models

The objective of the proposed model order reduction technique is to obtain low order models suitable for the design of an active aeroservoelastic control law that also performs well on the original system. It is therefore more important to ensure that resulting closed-loop systems behave similarly than to find an approximation for the open-loop model. The commonly used $\mathcal{L}_\infty$ norm, i. e., $\|P_1 - P_2\|_\infty$, thus does not appear particularly useful for evaluating the success of model reduction in this context. Further, since aeroservoelastic systems exhibit several very lightly damped modes, the $\mathcal{L}_\infty$ norm is very sensitive to small frequency shifts, cf. Ref 7.

Instead, the ν-gap metric $\delta_\nu(\cdot,\cdot)$ is used as a measure since it takes into account the feedback control objective. It takes values between zero and one, where zero is attained for two identical systems. A system P_1 that is within a distance ϵ to another system P_2 in the ν-gap metric, i. e. $\delta_\nu(P_1, P_2) < \epsilon$, will be stabilized by any feedback controller that stabilizes P_2 with a stability margin of at least ϵ.[17] A plant at a distance greater than ϵ from the P_2, on the other hand, will in general not be stabilized by the same controller. The ν-gap metric thus captures the likelihood that a feedback controller designed on the ROM will perform well on the full order model. It can be calculated frequency by frequency as[18]

$$\delta_\nu(P_1(\mathrm{j}\,\omega)\,, P_2(\mathrm{j}\,\omega)) = \left\| (I + P_2(\mathrm{j}\,\omega)\; P_2^*(\mathrm{j}\,\omega))^{-1/2}\; (P_1(\mathrm{j}\,\omega) - P_2(\mathrm{j}\,\omega))\; (I + P_1^*(\mathrm{j}\,\omega)\; P_1(\mathrm{j}\,\omega))^{-1/2} \right\|_\infty \tag{14}$$

Since the interpolated LPV model exactly reproduces the reduced LTI models at the grid points, the only potential problems may arise in between grid points. To show that the modal matching indeed yields a smooth interpolated model, linear interpolation with a grid density of 0.1 knots is performed. Figure 4 shows the frequency-dependent ν-gap metric of the LPV reduction model and the modal matching reduction model with respect to the full order 148 state model evaluated at all interpolation points. The overall accuracy of both ROMs is very good within the frequency range of interest. The ν-gap values are well below 0.2 at frequencies up to 160 rad/s and equal 0.3 at 200 rad/s for both cases. The LPV model reduction leads to a smaller error at high airspeed and low frequency, but to a larger error at low airspeed when compared to the interpolated model. Within the critical frequency range of about 40–80 rad/s, where the unstable modes are located, the interpolated model is more accurate than the LPV model. The ν-gap varies smoothly across the airspeed dimension for both ROMs. With the LMI-based approach explicitly accounting for the parameter dependence, this is to be expected. The proposed method, however, yields similarly smooth results between grid points. All ν-gap values for the interpolated models are extremely close to the LTI results as confirmed by figure 3(b).

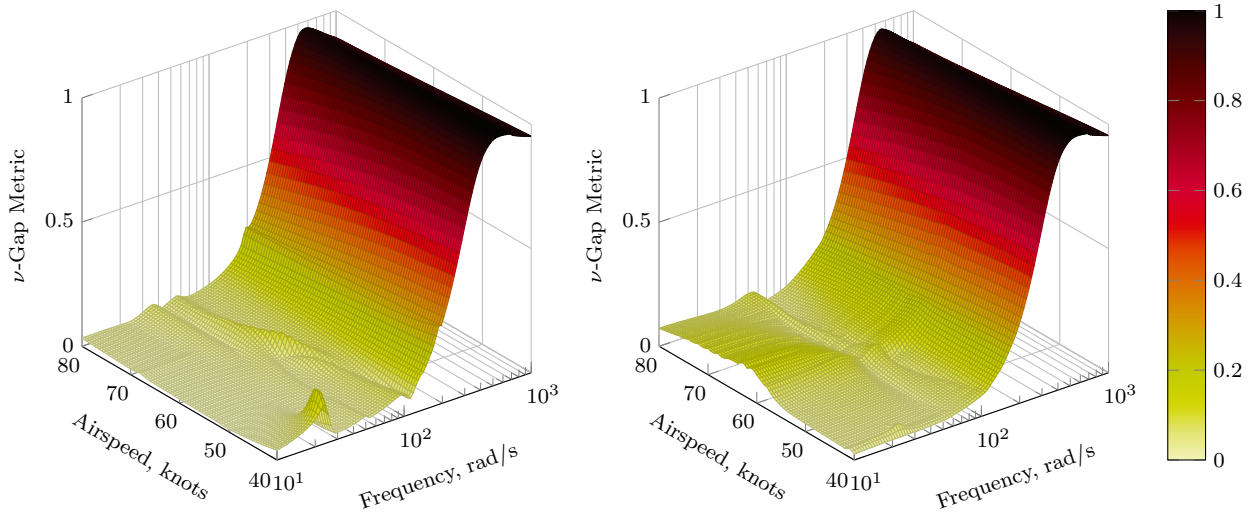

(a) LMI-based model reduction (26 states)

(b) Proposed method (15 states)

Figure 4. Variation of the ν-gap between the reduced order models and the full order model (148 states).

Pole migration within the frequency range of interest is shown in figure 5 for the full order model and the ROM with 15 states. Again, smoothness of interpolation is confirmed. Further, the evolution of the modes that become unstable can be seen to be captured very accurately.

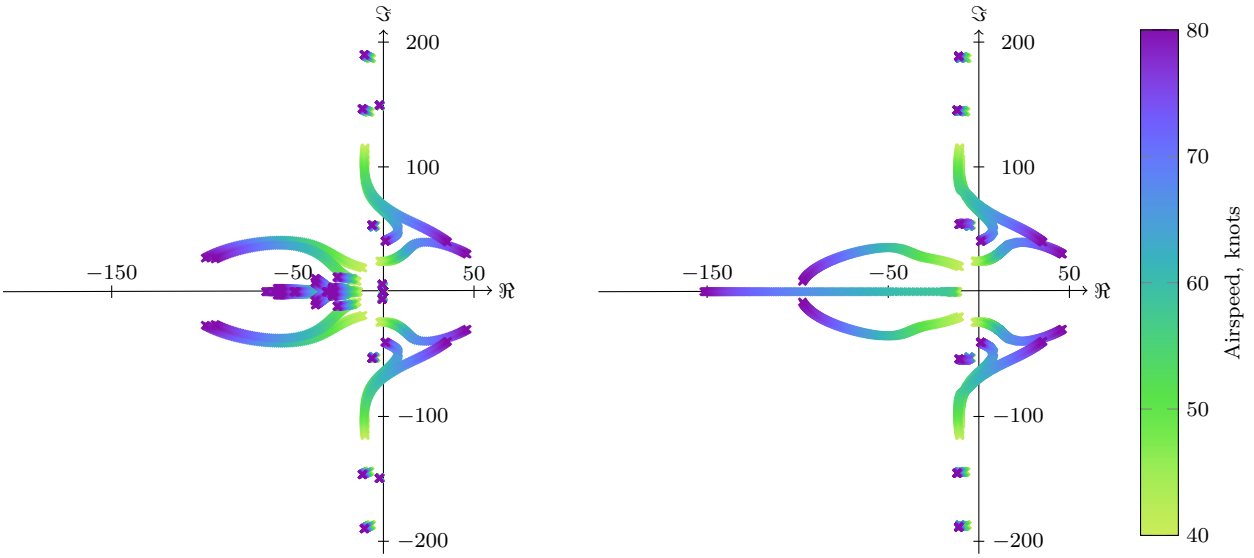

(a) Full order model (148 states)

(b) Reduced order model (15 states) with proposed method

Figure 5. Pole migration across the flight envelope.

Figure 6 depicts Bode plots for airspeeds not included in the original grid and obtained by linear interpolation. Both ROMs capture the input-output behavior of the full order model very well in the frequency range of interest. The LMI-based ROM can be observed to yield a slightly larger resemblance in the Bode plots of the starboard wing forward measurement, figures 6(a–b). Both ROMs appear to be least accurate for the body forward sensor measurement, figures 6(e–f).

V. Conclusions and Future Work

The proposed ROM with 15 states achieves the same level of accuracy as the 26th order model obtained by LMI-based reduction techniques in the ν-gap metric and comparable resemblance of the Bode plots. The additional 40% decrease in the number of states while maintaining this accuracy shows the potential benefits of using local transformations over parameter-independent ones. Numerical issues and high computational cost associated with LMI techniques are further completely avoided. Evaluation on a dense grid confirms that the proposed method indeed yields a smooth LPV model. The ν-gap metric between the full order and the proposed ROM is below 0.2 everywhere in the frequency range of interest and all unstable modes of the Body Freedom Flutter Vehicle are captured accurately. Therefore, and with its much lower dynamic order, the proposed ROM is expected to be well suited for control design.

Designing a controller based on the ROM and validating it on the full order model is a necessary next step in order to confirm this. Since the proposed method requires all locally reduced models to have the same number of complex and real poles, future work will also focus on finding methods to guarantee that this constraint is fulfilled in the local reduction or to modify the matching procedure to deal with a varying number. Finally, error bounds are to be developed to quantify the approximation error within the LPV framework, dependent on the neglected parameter variation rates.

VI. Acknowledgment

This work is partially supported by the NASA Phase II SBIR contract No. A2.04-8418 entitled *Reduced Order Aeroservoelastic Models with Rigid Body Modes* as a subcontract from Systems Technology Inc. Dr. Peter Thompson is the principal investigator and Dr. Martin Brenner is the NASA technical monitor.

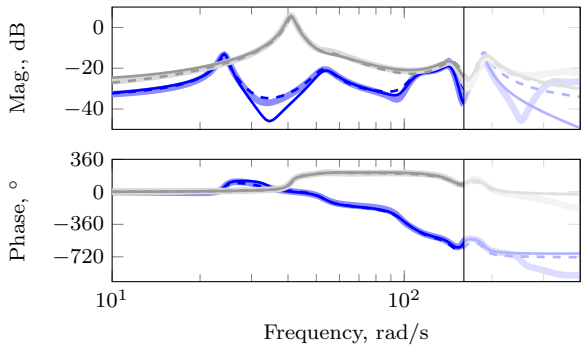

(a) From starboard body flap to starboard wing forward

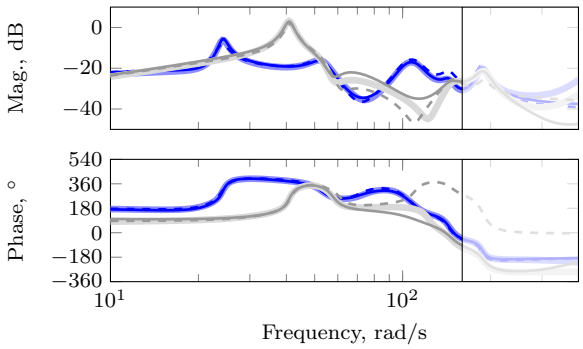

(b) From port outboard flap to starboard wing forward

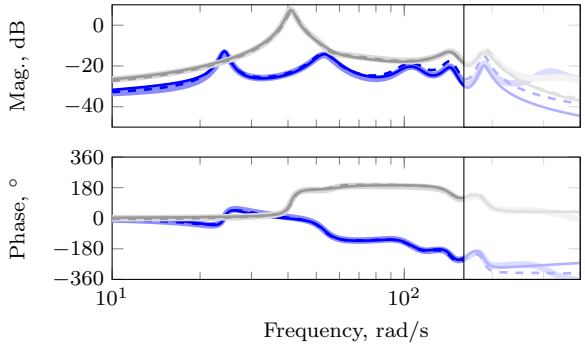

(c) From starboard body flap to starboard wing aft

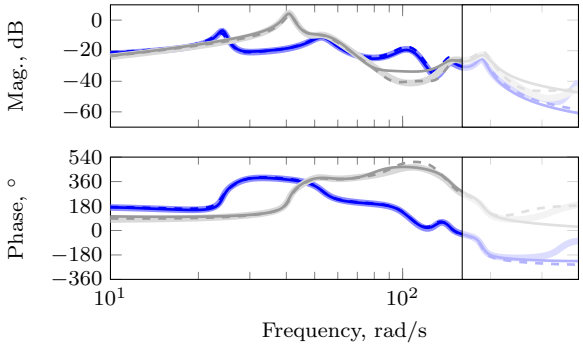

(d) From port outboard flap to starboard wing aft

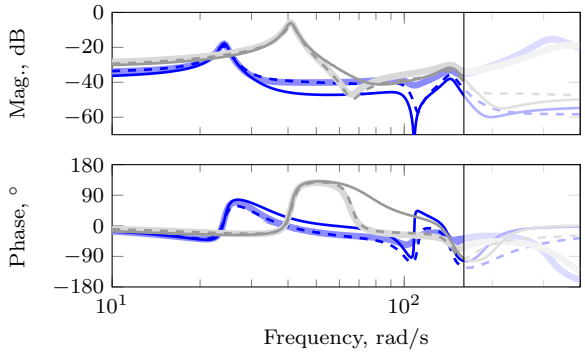

(e) From starboard body flap to body forward

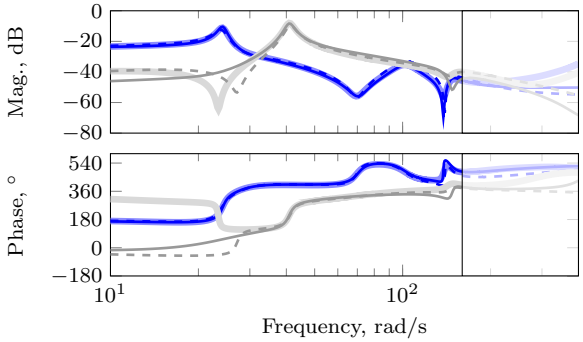

(f) From port outboard flap to body forward

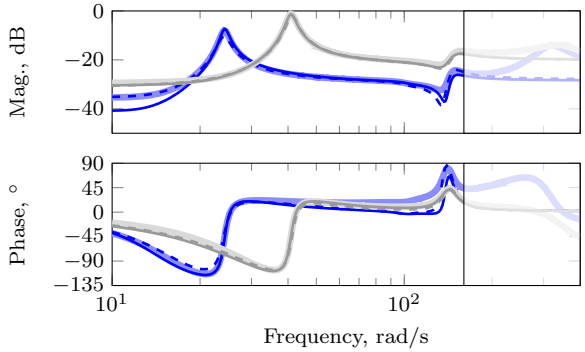

(g) From starboard body flap to body aft

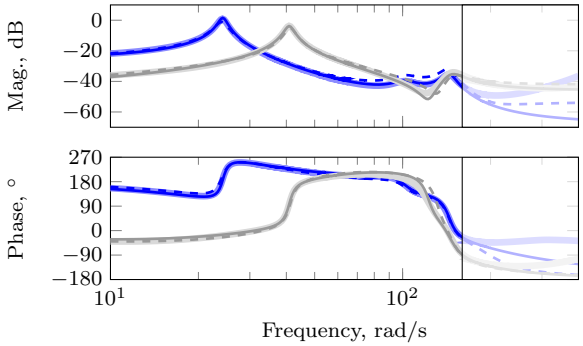

(h) From port outboard flap to body aft

Figure 6. Bode plots of full order model (148 states) at 43 knots (▬) and 77 knots (▬) compared to the proposed reduced order model with 15 states (▬/▬) and LMI-based reduced order model with 26 states (▬ ▬/▬ ▬). The lightened area denotes the frequency range beyond interest.

References

[1]Lind, R. and Brenner, M., *Robust Aeroservoelastic Stability Analysis*, Springer, 1999.

[2]Caldwell, B. D., Pratt, R. W., Taylor, R., and Felton, R. D., *Flight Control Systems: Practical Issues in Design and Implementation*, chap. Aeroservoelasticity, Stevenage IET, 2000, pp. 225–301.

[3]Wright, J. R. and Cooper, J. E., *Introduction to Aircraft Aeroelasticity and Loads*, John Wiley & Sons, 2007.

[4]Shamma, J. S., *Analysis and Design of Gain Scheduled Control Systems*, Ph.D. thesis, Massachusetts Institute of Technology, 1988.

[5]Becker, G., *Quadratic Stability and Performance of Linear Parameter Dependent Systems*, Ph.D. thesis, University of California, Berkeley, 1993.

[6]Wood, G. D., *Control of Parameter-Dependent Mechanical Systems*, Ph.D. thesis, Univ. Cambridge, 1995.

[7]Moreno, C. P., Seiler, P., and Balas, G., "Model Reduction for Aeroservoelastic Systems," *Journal of Aircraft*, Vol. 51, No. 1, 2014.

[8]Zhou, K., Doyle, J. C., and Glover, K., *Robust and Optimal Control*, Prentice Hall, Upper Saddle River, NJ, 1995.

[9]Skogestad, S. and Postlethwaite, I., *Multivariable Feedback Control*, Prentice Hall, Upper Saddle River, NJ, 2005.

[10]Antoulas, A., *Approximation of Large-Scale Dynamical Systems*, Society for Industrial and Applied Mathematics, Philadelphia, PA, 2005.

[11]Poussot-Vassal, C. and Roos, C., "Generation of a Reduced-Order LPV/LFT Model from a Set of Large-Scale MIMO LTI Flexible Aircraft Models," *Control Engineering Practice*, Vol. 20, 2012, pp. 919–930.

[12]Caigny, J. D., Camino, J. F., and Swevers, J., "Interpolation-Based Modeling of MIMO LPV Systems," *IEEE Transactions on Control Systems Technology*, Vol. 19, No. 1, 2011, pp. 46–63.

[13]Panzer, H., Mohring, J., Eid, R., and Lohmann, B., "Parametric Model Order Reduction by Matrix Interpolation," *Automatisierungstechnik*, Vol. 8, 2010, pp. 475–484.

[14]Kailath, T., *Linear Systems*, Prentice Hall, Englewood Cliffs, NJ, 1980.

[15]Holm-Hansen, B., Atkinson, C., Beranek, J., Burnett, E., Nicolai, L., and Youssef, H., "Envelope Expansion of a Flexible Flying Wing by Active Flutter Suppression," *AUVSI Unmanned Systems North America Conference*, Denver, CO, 2010.

[16]Safonov, M. and Chiang, R., "A Schur Method for Balanced Model Reduction," *IEEE Transactions on Automatic Control*, Vol. 34, No. 7, 1989, pp. 729–733.

[17]Vinnicombe, G., *Measuring Robustness of Feedback Systems*, Ph.D. thesis, University of Cambridge, 1993.

[18]Zhou, K. and Doyle, J. C., *Essentials of Robust Control*, Prentice Hall, Upper Saddle River, NJ, 1998.